
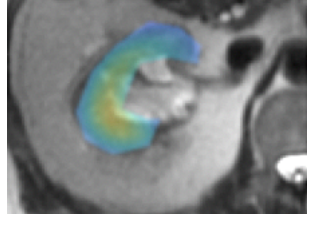
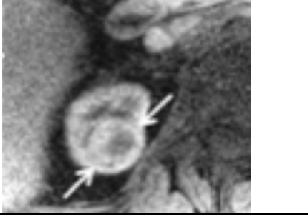
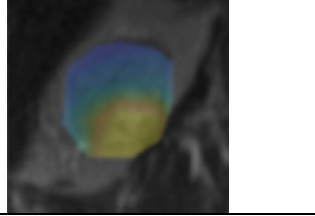
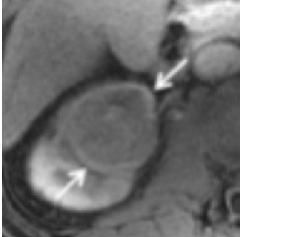
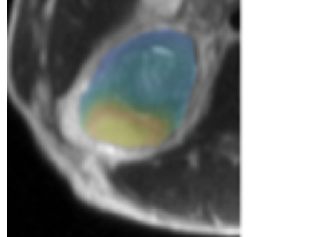
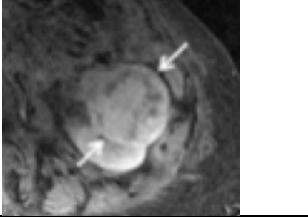
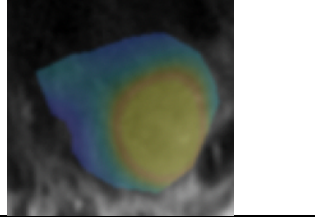
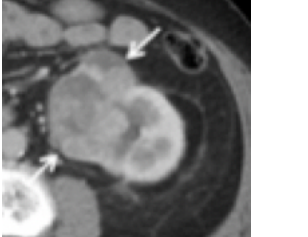
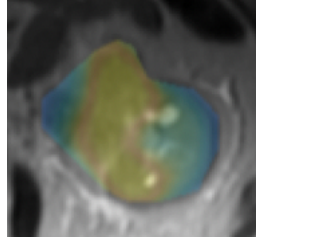
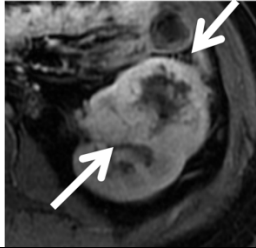
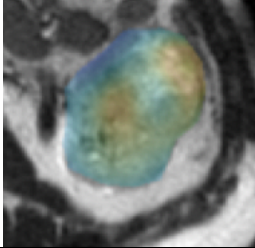

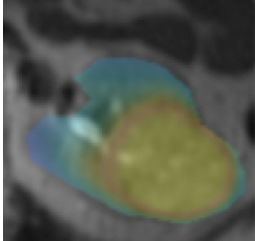

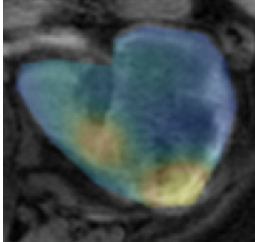
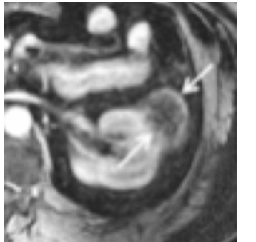
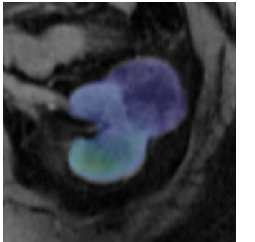

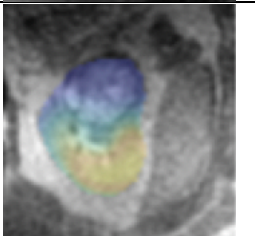


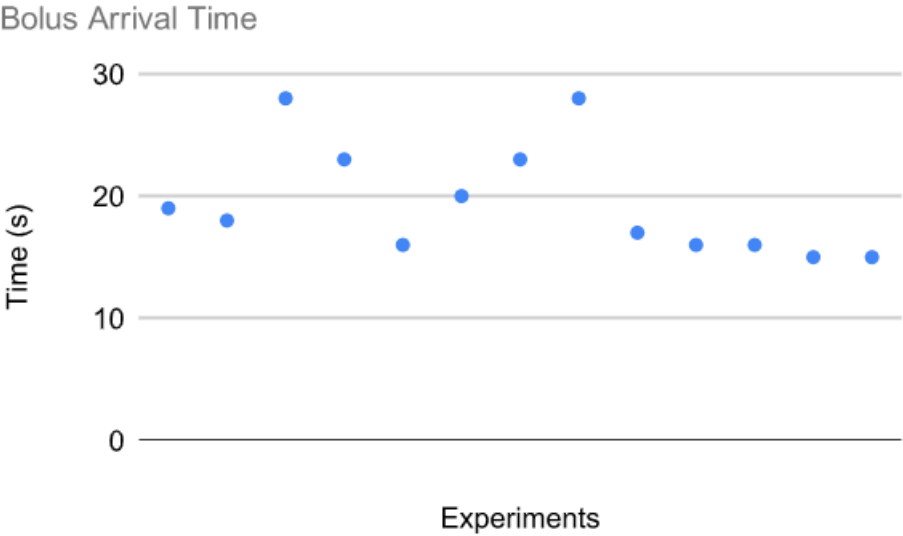
Supporting Figure 1. Gadolinium enhanced MRI images or contrast enhanced CT images as well as hyperpolarized ^{13}C pyruvate AUC images of renal tumors in patients enrolled in the study. The patient numbering corresponds to that in Table 1. The two cases excluded from the data analysis (last 2 rows) show very low level of perfusion on the gadolinium enhanced images, which likely contributes to the very low SNR on the hyperpolarized ^{13}C pyruvate images.

Patient	Gadolinium enhanced MRI images or contrast enhanced CT images	^{13}C pyruvate images	Pathology
1			Chromophobe RCC
2			Clear Cell RCC (grade 2)
3			Chromophobe RCC
4			Clear cell RCC (grade 2)
5			Clear cell RCC (grade 3)

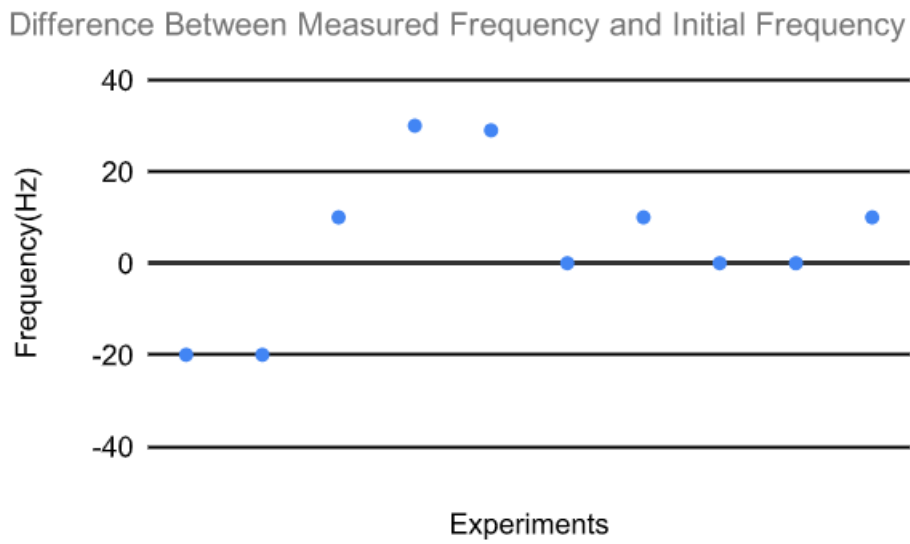
6			Clear cell RCC (grade 4)
7			Clear cell RCC (grade 2)
8			Clear cell RCC (grade 3)
Excluded case -1			Clear cell RCC (grade 2)
Excluded case -2			Clear cell RCC (grade 2)



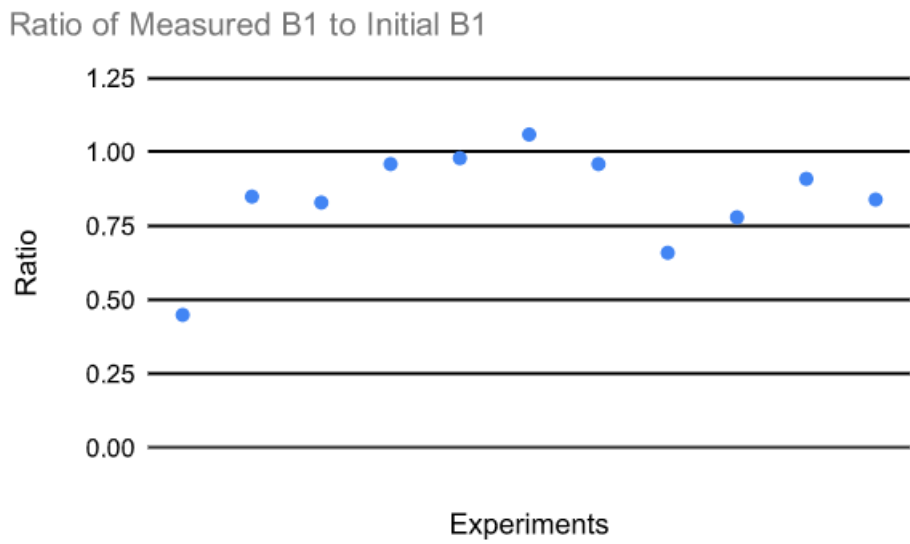
Supporting Figure 2. Bolus arrival time in the kidneys from the beginning of injection.



Supporting Figure 3. Real-time measured frequency (**A**) and power (**B**).
A)



B)



Supporting Figure 4. Area-under-the-curve (AUC) images from hyperpolarized ^{13}C pyruvate MRI in patient where ^{13}C images were acquired for both kidneys. For patients 1, 3 and 6, ^{13}C images were only acquired of the kidney containing tumor, as patient 3 had a solitary tumor, and patient 1 and 6 had tumors that were located more laterally and anteriorly (thus instead of placing the second paddle coil posteriorly to the contralateral kidney, the coil was placed anterior-laterally over the side containing the tumor).

